International Journal of Pharmaceutics 668 (2025) 124970

Contents lists available at ScienceDirect

International Journal of Pharmaceutics

journal homepage: www.elsevier.com/locate/ijpharm

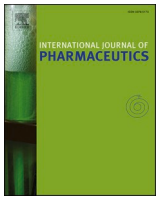

Human and canine osteosarcoma cell lines: How do they react upon incubation with calcium phosphate-coated lipid nanoparticles carrying doxorubicin and curcumin?

Simona Sapino [a,1], Elena Peira [a,1], Daniela Chirio [a,*], Giulia Chindamo [a], Giulia Accomasso [a], Cristina Vercelli [b,*], Chiara Riganti [c], Iris Chiara Salaroglio [c], Graziana Gambino [b], Giovanni Re [b], Michela Amadori [b], Marina Gallarate [a]

[a] Department of Drug Science and Technology, Turin University, Via P. Giuria 9, 10125 Torino, Italy
[b] Department of Veterinary Sciences, Turin University, Largo Paolo Braccini 2, 10095 Grugliasco, Torino, Italy
[c] Department of Oncology, Turin University, Piazza Nizza 44, 10126, Torino, Italy

ARTICLE INFO

Keywords:
Lipid nanoparticles
Osteosarcoma
Doxorubicin
Curcumin
Multidrug resistance
In vitro cell studies

ABSTRACT

Osteosarcoma (OSA) is a bone cancer that affects both humans and animals, with dogs being particularly vulnerable. Standard therapy is often limited by multidrug resistance (MDR), primarily due to the overexpression of P-glycoprotein (P-gp), which expels drugs from the cells, reducing their efficacy. To overcome this challenge, drug delivery systems (DDS) and P-gp modulators have been explored. However, developing DDS that selectively target cancer cells remains difficult, with many current options lacking efficiency. Our research group has recently developed an innovative type of nanoparticle with a lipid core and a calcium phosphate shell (CaP-NPs), which enhances the uptake of doxorubicin (DOXO) in OSA cells. In this study, we loaded a lipophilic ester of doxorubicin (C12DOXO) and curcumin (CURC), a natural P-gp modulator, into CaP-NPs and co-incubated them into human and canine OSA cell lines, including DOXO-resistant cells. The results demonstrated a significant reduction in viability in human OSA cells. Additionally, the combination treatment led to a further increase in C12DOXO retention when cells were also treated with the P-gp inhibitor verapamil, indicating enhanced efficacy against MDR mechanisms. Notably, canine OSA cells exhibited a distinct response pattern, suggesting the presence of species-specific differences that warrant further investigation.

1. Introduction

Osteosarcoma (OSA) is the most common form of malignant bone tumor in both humans and dogs. It is a highly aggressive cancer, characterized by rapid progression and a high propensity for metastasis, particularly to the lungs. OSA accounts for the majority of primary bone malignancies in both species and has a poor prognosis despite intensive treatment efforts. Current standard treatment typically involves a multimodal approach combining surgical resection of the primary tumor with chemotherapy to manage micrometastatic disease and improve overall survival rates (Ta et al., 2009; Makielski et al., 2019).

One of the standard chemotherapeutic agents used in OSA treatment is doxorubicin (DOXO), an anthracycline antibiotic that intercalates DNA and disrupts vital cellular processes, leading to cancer cell death (Kciuk M et al.; 2023). Despite its effectiveness, DOXO induces systemic toxicity that affects multiple organs, such as dose-dependent cardiotoxicity; therefore, its use is significantly limited by such dose-limiting toxicities, (Sheibani et al., 2022), and by the development of multidrug resistance (MDR) in tumor cells. One of the primary mechanisms of MDR involves the overexpression of P-glycoprotein (P-gp), which actively exports chemotherapeutic drugs, reducing their intracellular concentration and efficacy (Garcia-Ortega et al., 2022).

* Corresponding authors.
E-mail addresses: simona.sapino@unito.it (S. Sapino), elena.peira@unito.it (E. Peira), daniela.chirio@unito.it (D. Chirio), giulia.chindamo@unito.it (G. Chindamo), giulia.accomasso@unito.it (G. Accomasso), cristina.vercelli@unito.it (C. Vercelli), chiara.riganti@unito.it (C. Riganti), irischiara.salaroglio@unito.it (I.C. Salaroglio), graziana.gambino@unito.it (G. Gambino), giovanni.re@unito.it (G. Re), michela.amadori@unito.it (M. Amadori), marina.gallarate@unito.it (M. Gallarate).
[1] These authors contributed equally to this work.

https://doi.org/10.1016/j.ijpharm.2024.124970
Received 25 July 2024; Received in revised form 15 November 2024; Accepted 16 November 2024
Available online 19 November 2024

Therefore, overcoming the adverse reactions and resistance mechanisms of DOXO is critical for developing more effective therapeutic strategies for OSA patients (Li et al., 2015).

Recent advances in drug delivery systems (DDS) offer a promising approach to enhance the effectiveness of chemotherapeutic agents while minimizing systemic toxicity (Sun et al., 2024). Successful drug delivery demands that therapeutic agents be released at specific target sites in a controlled manner, maximizing therapeutic efficacy while minimizing adverse reactions. DDS, including liposomes and micelles, help protect drugs from rapid degradation, increase efficacy, and reduce adverse reactions by targeting the drug directly to tumor sites both by passive and/or active targeting, the latter achieved by functionalizing DDS with targeting ligands further improves selectivity, minimizing the impact on healthy tissues (Rana et al., 2023). Moreover, they can promote endocytosis-based entry into tumor cells, reducing dependence on passive diffusion pathways typically targeted by P-gp.

In the context of OSA treatment, nanoparticulate DDS have shown promise in overcoming DOXO resistance. Susa et al. (2009) demonstrated that DOXO-loaded lipid-modified dextran nanoparticles (NPs) were effective in both drug-sensitive and drug-resistant OSA cell lines by enhancing drug accumulation through P-gp-independent pathways, resulting in increased apoptosis and improved treatment efficacy. A subsequent study by Susa et al. (2010) used NPs to deliver MDR1-targeting siRNA, successfully suppressing P-gp expression and reversing drug resistance in MDR-OSA cell lines.

To further enhance DOXO efficacy and reduce cardiotoxicity, Gazzano et al. (2019) developed synthetic DOXO conjugated with an H_2S-releasing moiety, which proved less cardiotoxic and more effective against P-gp-overexpressing OSA cells when loaded into hyaluronic acid (HA)-conjugated DOXO liposomes (HCDL). The HCDL formulation demonstrated superior drug release profiles and exhibited increased toxicity *in vitro* and in *vivo* compared to DOXO or the FDA-approved liposomal DOXO, Caelyx®. These results suggest HCDL as a promising approach for further investigation in patients with P-gp-overexpressing tumors.

Another strategy to overcome MDR is leveraging drug synergy within DDS. For instance, co-delivery of curcumin (CURC), a natural polyphenol with P-gp inhibitory properties, with DOXO has been shown to exert a synergistic effect by enhancing chemotherapy effectiveness. Duan et al. (2012) and Wang et al. (2016) demonstrated that the co-encapsulation of DOXO and CURC in NPs reversed MDR in resistant cancer cell lines, resulting in significantly higher cytotoxicity compared to both drugs alone. In a clinical study, Lu et al. (2024) showed that co-delivery of DOXO and CURC in lipid NPs reduced side effects and renal function damage in OSA patients undergoing preoperative chemotherapy, suggesting a promising strategy for improving treatment efficacy and safety.

Despite these advances, a significant challenge remains in effectively targeting tumor tissues and achieving sufficient accumulation of nanocarriers at OSA sites while minimizing off-target effects. NPs with a calcium phosphate (CaP) shell offer particular advantages for treating bone-related diseases like OSA due to their biocompatibility and osteoconductivity, which facilitate improved localization to bone tumors and enhance drug delivery efficiency. In our previous work (Sapino et al., 2021), CaP-coated NPs demonstrated superior cellular uptake in both human and canine OSA cells compared to uncoated NPs, suggesting that CaP improves internalization.

Building on these findings, our group developed CaP-coated NPs loaded with a lipophilic ester of DOXO (C12DOXO), demonstrating increased uptake and cytotoxicity in OSA cells, particularly in the presence of external calcium ions. This approach holds potential for enhancing targeted OSA treatment by improving drug accumulation in cancer cells (Chirio et al., 2022).

In the present study, we aim to leverage the potential of CaP-coated NPs in combination with the synergistic effects of DOXO and the natural P-gp inhibitor CURC to inhibit resistance in both human and canine OSA. Specifically, we developed CURC-loaded CaP-NPs and evaluated their potential for co-incubation with C12DOXO-loaded CaP-NPs in drug-sensitive and drug-resistant human and canine OSA cell lines. By incorporating CURC into CaP-coated NPs, we aim to exploit its resistance-inhibiting properties, enhancing the therapeutic efficacy of C12DOXO and providing insights into treatment responses across species.

2. Materials and Methods

2.1. Chemicals

Doxorubicin (DOXO), dodecanoic acid, trilaurin, curcumin (CURC), ethyl acetate (EA), sodium hydroxide, propylene glycol, calcium chloride, sodium phosphate dibasic dihydrate, Sepharose®CL4B, were purchased from Sigma Aldrich (St. Louis, MO, USA). Epikuron®200 (soybean lecithin, containing 95 % phosphatidylcholine) from Cargill (Minneapolis, MN, USA); Cremophor®RH60 (PEG-60 hydrogenated castor oil) by Acef (Piacenza, Italy); sodium chloride and phosphoric acid from Alfa Aesar (Haverhill, Massachusetts, USA).

2.1.1. Synthesis and characterization of the lipophilic derivative of DOXO

The lipophilic derivative C12DOXO was synthesized by esterification of DOXO with dodecanoic acid and then characterized as reported in our previous work (Peira et al., 2016).

2.2. Preparation of NPs

Blank NPs and NPs loaded either with C12DOXO or with CURC were prepared with the previously developed "cold microemulsion dilution" method (Chirio et al., 2019). More precisely, to obtain the lipid phase, the lipid matrix was solubilized in 200 μL of water-saturated EA (s-EA), along with appropriate amounts of surfactant and cosurfactant. Afterwards, 700 μL of EA-saturated water (s-water) were added dropwise to the lipid phase, and then vortexed at room temperature until an oil-in-water microemulsion (μE) was obtained. Subsequently, 5 mL of water were added to the μE at room temperature, facilitating the diffusion of the organic solvent from the inner phase into the added water, resulting in the precipitation of solid lipid nanoparticles (NPs). The ionized phosphate group of Epikuron®200 was exploited to impart a negative charge on the surface of the NPs, which is necessary to ensure the coating process. The same method was also used to prepare C12DOXO loaded NPs and CURC loaded NPs. Different amounts of the drugs were dissolved in the lipid phase.

Table 1 reports the compositions of blank NPs, C12DOXO-loaded NPs, and of NPs loaded with increasing amounts of CURC.

2.3. Purification of NPs

Gel filtration was used to purify NPs employing a crosslinked agarose matrix (Sepharose ®CL4B) as the stationary phase and PBS as the mobile phase. An aliquot (0.5 mL) of NPs suspension was first subjected to gel filtration and the resulting opalescent fraction (3 mL) containing the purified NPs was then dialyzed for 2 h at room temperature against ultrapure water using a dialysis bag (MWCO = 14,000 Da) in order to remove excess salts and unloaded molecules. The same procedure was adopted for C12DOXO NPs and CURC NPs.

2.4. Coating technique

NPs were coated with CaP according to the procedure described in our previous paper (Sapino et al., 2021). Briefly, aliquots of Na_2HPO_4 and $CaCl_2$ salt solutions were added to the purified NPs. The two different salts have been sequentially added and alternating the aliquots in a layer-by-layer process. To ensure two negative charges on the phosphate group, pH was monitored and maintained around 8.5 during

Table 1
Compositions of blank and loaded μEs, and of the resultant NPs (*water-saturated ethyl acetate; **dodecanoyl-doxorubicin ester; ***curcumin).

		Ingredients	μE0/NP0	μED6/NPD6	μEC5/NPC5	μEC7.5/NPC7.5	μEC10/NPC10
NANO PARTICLES	**MICRO EMULSIONS**	Trilaurin (mg)	60	60	45	45	45
		s-EA* (μL)	200	200	200	200	200
		Epikuron®200 (mg)	170	170	180	180	180
		Cremophor®RH60 (mg)	50	35	35	35	35
		Propylene glycol (μL)	100	90	100	120	160
		s-Water (μL)	700	700	700	700	700
		C12DOXO** (mg)	–	6	–	–	–
		CURC*** (mg)	–	–	5	7.5	10
		Dilution water (mL)	5	5	5	5	5

each addition. The resulting CaP-NPs suspensions were then dialyzed overnight at room temperature against ultrapure water with a 14,000 Da MWCO to remove the excess ions.

2.5. Characterization of NPs

NPs have been accurately characterized using a number of different techniques, including measuring their size and surface characteristics and testing their loading efficiency.

2.5.1. Mean diameter and surface charge

Dynamic light scattering (DLS) instrument (Brookhaven Instruments, Holtsville, NY, USA) was employed to perform the measurements. Mean diameters of NPs were determined in triplicate. Surface charge measurements were conducted using Zeta potential mode. In both measurements, ultrapure water was used to dilute samples, and ten measurements were taken to determine Zeta potential.

2.5.2. HPLC analyses

HPLC analyses were conducted using a Shimadzu HPLC system (Tokyo, Japan) equipped with a C-R5A integrator and a Teknokroma® ODS column (5 μm, 15 cm × 0.46 cm). C12DOXO was eluted using a gradient method with a mobile phase consisting of 0.3 % H_3PO_4 in water and 0.1 % H_3PO_4 in CH_3CN, at 1.0 mL/min flow rate. Detection was performed fluorometrically with excitation at λ480 nm and emission at λ 520 nm, following a previously described procedure [10]. CURC HPLC analysis was performed using a Teknokroma®ODS column (5 μm, 15 cm × 0.46) and a Shimadzu (Tokyo, Japan) HPLC apparatus; the detection was performed with UV–Vis detector, λ 450 nm (Shimadzu, Tokyo, Japan). CURC was eluted in isocratic conditions at 1.0 ml/min flow using CH_3OH/3.5 % CH_3COOH in water (70:30 v/v) as mobile phase. A calibration curve was built by plotting the peak area as a function of drug concentration. An acceptable linearity ($R^2 = 0.9999$) was obtained in the 5–100 μg/mL range. The relative standard deviation (RSD) of intra-and inter-day precision for 3 concentrations (10, 20 and 50 μg/mL) was below 3 % with accuracy ranging from 97.0 % to 103.0 %. As CURC is a fluorescent molecule, to verify shape and drug entrapment CURC-NPs were observed by an optical microscope (Leica DM 2500, Solms, Germany) equipped with a fluorescent lamp at 1000 X magnification.

2.5.3. Entrapment efficiency Evaluation

Entrapment efficiency percentages (%EE) of either C12DOXO or CURC in the developed NPs were investigated using a gel chromatography column of Sepharose®CL4B. Fixed aliquots of the prepared NPs suspension were carefully loaded onto the column and then eluted with pH 7.4 PBS as mobile phase. Fractions were collected in tubes and analyzed by HPLC. Each value of %EE was obtained by dividing the amount of drug found in the filtrated fractions of the NPs by the total amount of drug added in the preparation of NPs, and then multiplying the result by 100.

2.5.4. Freeze-Drying/Re-Suspension of NPs

CaP-NPs suspensions were freeze-dried either in the absence or in the presence of a cryoprotectant (10 % w/v trehalose or glucose or sucrose) in order to increase their long term storage. All the samples were stored at −40 °C overnight and then dried under 50 mtorr atmosphere for 24 h. Finally, NPs were reconstituted in milliQ water under agitation. Mean diameter, polydispersity index, and Zeta potential of the reconstituted samples were determined.

2.5.5. In vitro release study

The release of CURC from NPs was determined *in vitro* employing a multi-compartment rotating cell system. Several donor and receptor compartments of equal volume (1.5 mL) were separated by a hydrophilic membrane, Servapor® dialysis tubing (Serva, Heidelberg, Germany), cut-off 12,000–14,000 Da (Trotta et al., 2004). In separate experiments, 10 % PEG 300 CURC solution, NPC10, and CaP-NPC10 suspensions were used as donor formulations. 10 % PEG 300 water solution (pH 7.8) was employed as the receiving medium. To mimic sink conditions, at fixed times, the receiving solution was fully removed and the compartment was filled with fresh receiving medium. CURC concentration in the receiving medium was determined by HPLC. The release of C12DOXO systems was already studied in a previous work (Chirio et al., 2022).

2.6. In vitro cell studies

2.6.1. Human osteosarcoma and osteoblast cells

Human DOXO-sensitive osteosarcoma U-2OS cells (HTB-96, ATCC, Manassas, VA, USA) were cultured at 37 °C, 5 % CO_2, in Dulbecco's modified Eagle's medium (DMEM) (Invitrogen, Milan, Italy), containing 1 % v/v penicillin–streptomycin (Sigma-Merck, St. Louis, MO, USA) and 10 % v/v foetal bovine serum (FBS) (Sigma-Merck). The DOXO-resistant counterpart cells (U-2OS/DX) were generated by culturing U-2OS cells in medium with increasing concentrations of DOXO up to 580 ng/mL DOXO (Serra et al., 1993), used as "maintenance concentration". Human non– transformed osteoblasts were generated as previously described (Buondonno et al, 2016): mesenchymal stem cells from healthy volunteers were cultured in differentiation osteogenic medium for 14 days (Gronthos et al., 2003). The osteoblast differentiation was confirmed by the Bone Alkaline Phosphatase (Sigma-Merck), as per manufacturer's instructions, then used for the experiments reported.

2.6.2. Canine osteosarcoma D17 cells

Canine osteosarcoma D17 cells (CRL-8468, ATCC, Manassas, VA, USA) were cultured at 37 °C and 5 % CO_2 atmosphere in the presence of complete medium composed of DMEM, 10 % v/v FBS, 2 % v/v antibiotic and antimycotic solution, and 2 % v/v L-glutamine. All reagents were purchased from Sigma Aldrich (Merck company, St. Louis, MO, USA).

2.6.3. Cytotoxicity assay

The cytotoxicity assay was performed on both human and canine OSA cells according to Vercelli et al. (2014) on 5 × 10^3 cells/100 μL cells, seeded in 96-well plates, incubated for 72 h. First, to determine IC50 values, U-2OS, U-2OS/DX and D17 cells were incubated separately with free C12DOXO and CURC at concentrations ranging from 0.01 μM

to 100 μM. Then, U-2OS and U-2OS/DX cells were incubated with C12DOXO 2.5 μM, CURC 22 μM, CaP-NPD6 2.5 μM, CaP-NPC10 22 μM, and their combinations; D17 cell line was incubated with C12DOXO 59 μM, CURC 16 μM, CaP-NPD6 59 μM, CaP-NPC10 16 μM, and their combinations. In parallel, cells were incubated for 72 h with blank NPs (CaP-NP0), choosing the lipid concentration corresponding to the minimum dilution used when CaP-NPC10 and CaP-NPD6 were co-administered. At the end of the incubation time, 20 μL of the 3-(4,5-dimethylthiazol-2-yl)-2,5-diphenyltetrazolium bromide (MTT) solution (5 mg/mL in PBS) were added to each well and the plates were incubated for 4 h at 37 °C. Then, the content of wells was removed and 150 μL of DMSO were added to allow dissolution of precipitated formazan salt, maintaining the plates under shaking for 10 min at room temperature. The absorbance was read using a plate reader (Poverwave x; Bio-Tek Instruments Inc., Winooski, USA) at 570 nm. Results were expressed as the percentage of viable cells, comparing the results obtained per each well of treated cells with the mean value of control (untreated) cells, and subtracting blank values. Each experimental condition was performed in quintuple. As a second read-out of cell viability, we used the ATPLite kit (PerkinElmer, Waltham, MA) as per manufacturer's instruction.

2.6.4. C12DOXO cellular uptake

Human cells, seeded in 24-well plates, were incubated for 24 h with C12DOXO 2.5 μM either free or entrapped in CaP-NPs (CaP-NPD6 2.5 μM) alone and in combination with CURC 22 μM or with CaP-NPC10 22 μM, respectively. Similarly, the canine cell line was incubated either with C12DOXO 59 μM free or entrapped in CaP-NPs (CaP-NPD6 59 μM) alone and in combination with CURC 16 μM or with CaP-NPC10 16 μM, respectively. In a further experimental setting, cells were co-incubated with the P-gp inhibitor verapamil 50 μM. At the end of the incubation times, cells were washed twice with PBS, detached with 0.50 μL trypsin, and re-suspended in 250 μL a 1:1 (v/v) solution of ethanol/HCl 0.3 N. An aliquot of 50 μL was sonicated and used for protein quantification using the BCA-1 kit (Sigma-Merck company, St. Louis, MO, USA). The remaining sample was transferred into a 96-well plate to measure the intracellular fluorescence of C12DOXO as an index of drug content, using a Synergy HTX multiplate reader (Bo-Tek Instruments, Winooski, VT), choosing excitation and emission wavelengths of 596 and 615 nm, respectively. Fluorescence units were converted to nmoles of C12DOXO according to a titration curve performed with free C12DOXO solutions at the 1, 10, 100, 250, and 500 nmol/mL concentrations. Results were expressed as nmol/mg cellular proteins. As second assay of intracellular DOXO accumulation, we measured the drug content by flow cytometry (Buondonno, 2019): 250 × 105 cells, incubated as described above, were washed twice with PBS, detached by the Cell Dissociation Solution (Sigma-Merck) and analyzed by a Guava® easyCyte flow cytometer (Millipore, Bedford, MA, USA), using the InCyte software (Millipore).

2.6.5. Statistical analysis

Data about cell cultures have been organized using Excel software (Microsoft corporation,Redmond, WE, USA). Results were analyzed using One-way variance analysis (ANOVA) and Tukey's multiple comparison test, using the Prism software (v 6.01, GraphPad, Boston, MA, USA). The same software has been used to calculate IC50 employing the specific function. A p-value < 0.05 was noted as significant. All data were expressed as means ± standard deviation (SD).

3. Results and discussion

The primary cause of OSA therapy failure is attributed to the MDR mechanism, which reduces the effectiveness of many drugs against this cancer type. Consequently, DOXO requires high-dose administration to be effective, leading to adverse reactions in major organs, especially cardiotoxicity (Swain et al., 2003) and bone marrow suppression.

The use of NPs as DDS has been described as one of the effective approaches to overcome MDR (Barraud et al., 2005; Duggan and Keating, 2011) and consequently, to enhance drug accumulation in drug-resistant tumor cells. Endocytosis of NPs could lead to bypass the P-gp-dependent efflux, resulting in increased intracellular drug concentration and drug cytotoxicity (Petschauer et al., 2015). In our previous work (Chirio et al., 2022) C12DOXO-loaded NPs showed a higher drug accumulation in OSA cells compared to free drug, even higher when NPs were CaP-coated.

This work represents a step forward, as DOXO was co-administered with CURC, a molecule capable of modulating P-gp expression and function in MDR cell lines (Anuchapreeda et al., 2002; Xue et al., 2013; Tang et al., 2005).

In the case of OSA, several researchers have successfully demonstrated that CURC can induce apoptosis of cell line MG63, U-2OS and HOS through different signal pathways (Zhang et al., 2017; Walters et al., 2008; Lee et al., 2009) and can suppress the proliferation, invasion and metastasis spreading (Sun et al., 2019; Withers et al. 2018). Nevertheless, CURC as a free drug has low bioavailability after oral administration, limiting its use in cancer treatment.

In this study, CURC was loaded into CaP-NPs to address this limitation, then its effectiveness in treating OSA was tested on both human and canine cell lines by co-administering it with CaP-C12DOXO NPs.

3.1. Characterization of NPs

In Table 2 mean diameters, Zeta Potential and drug %EE were reported.

All uncoated NPs showed mean diameters in the 200–300 nm range, which increased upon drug entrapment. Sizes of CaP-coated NPs were slightly higher than the uncoated one, probably owing to the deposition of salts on the surface of NPs.

Zeta potentials of NP0 and CURC-NPs were negative, due to the ionized phosphate groups of Epikuron®200. To verify the coating formation, these values were determined also during and after the CaP coating process. As already observed in our previous work (Sapino et al., 2021), after each addition of salt a significant change in Zeta potential was noted (data not reported). In particular, a marked increase in Zeta potential was observed after $CaCl_2$ solution addition, while strong negative values were observed following the addition of Na_2HPO_4 solution. This alternation of charges during the coating process could be an indication of layer-by-layer deposition of the added ions on NPs' surface. As shown, all final Zeta potentials resulted only slightly negative with values between −1.7 and −4.3 mV.

The characterization data of C12DOXO-loaded NPs, already reported and discussed in a previous work (Chirio et al., 2022), showed a strongly positive value when 6 mg of C12DOXO was loaded into NPs. This value could be due to a not insignificant amount of the drug that might be adsorbed on the NP surface with protonated amino groups exposed outward. Also in this case, an alternation of Zeta potential values was noted. Furthermore, the coating formation was assessed by FESEM analysis.

In Table 2 the %EE of C12DOXO and of CURC in both uncoated and

Table 2
Mean diameter, Zeta potential and drug entrapment efficiency of different NPs.

	Mean diameter (nm)	Zeta Potential (mV)	C12DOXO %EE	CURC %EE
NP0	209.7 ± 2.8	− 23.5 ± 1.4	–	–
CaP-NP0	232.2 ± 4.0	− 1.6 ± 0.2	–	–
NPD6	282.7 ± 3.2	+12.7 ± 1.5	87.2 ± 2.9	–
CaP-NPD6	311.8 ± 6.3	+1.6 ± 2.0	74.2 ± 2.4	–
NPC5	278.5 ± 2.6	−16.8 ± 2.0	–	98.2 ± 3.5
CaP-NPC5	311.8 ± 7.5	−4.3 ± 1.7	–	73.5 ± 2.8
NPC 7.5	285.4 ± 13.4	−17.0 ± 2.6	–	98.3 ± 3.0
CaP-NPC7.5	321.5 ± 15.7	−9.0 ± 2.2	–	74.5 ± 2.5
NPC10	260.2 ± 32.1	−19.8 ± 1.8	–	86.6 ± 2.2
CaP-NPC10	289.9 ± 18.9	−1.7 ± 3.1	–	81.5 ± 2.8

coated NPs is also reported. %EE of both drugs in all uncoated NPs was in the 80–90 % range but it decreased by about 15–20 % after CaP coating; probably, a part of the drug was released during the agitation and dialysis processes. No evident differences in %EE were noted varying the CURC amount.

As CURC-NPs loaded with 10 mg of drug (NPC10) presented the lowest mean diameters and the highest drug loading in the CURC-NP series, they were chosen for the following *in vitro* studies.

NPC10 were observed by an optical microscope equipped with a fluorescent lamp to assess their shape and drug entrapment. In Fig. 1A and 1B micrographs of NPC10 and CaP-NPC10 are reported.

Due to their small sizes, both uncoated and coated NPs appear as fluorescent points. Notably, all NPs exhibit an almost spherical shape, are not aggregated, and contain CURC. These observations corroborate the data obtained from DLS and %EE analyses.

To increase NPs stability overtime, CaP-NPC10 were freeze-dried in the absence and in the presence of different cryoprotectants. In Table 3 mean diameters of freshly prepared and re-suspended freeze-dried CaP-NPC10 are reported.

Since NP aggregation was observed in the absence of cryoprotectants (with CaP-NPC10 showing mean sizes over 500 nm), adding cryoprotectants was necessary to preserve characteristics similar to those of freshly prepared NPs. The mean NP diameter remained comparable to the initial values when sucrose and glucose were used as cryoprotectants, whereas trehalose had no effect on NP aggregation. As a result, it appears that freeze-drying of CaP-NPC10 can increase its stability over time.

3.2. In vitro release study

A CURC release study was conducted on NPC10 and CaP-NPC10, using an aqueous CURC solution in 10 % w/w PEG 300 as a reference (Fig. 2). This setup allowed for a comprehensive comparison of the release profiles.

CURC solution and both NPC10 and CaP-NPC10 showed very different release profiles. CURC release from the solution showed a first order release profile: about 55 % of CURC was released within 3 days. A slower CURC release rate was noted from NPs: only 15 % was released within 3 days and a pseudo-zero-order kinetic was observed in this time interval. As no burst effect was observed with NPC10 and CaP-NPC10, we can hypothesize that CURC was entrapped into the lipid matrix

Table 3
Mean diameters of CURC loaded CaP-NPs before and after freeze-drying.

Sample	Before freeze-drying (nm)	After freeze-drying (nm)
CaP −NPC10	289.9 ± 18.9	546.8 ± 7.6
CaP-NPC10 + 10 % threalose	289.9 ± 18.9	624.8 ± 44.0
CaP-NPC10 + 10 % sucrose	289.9 ± 18.9	318.1 ± 18.4
CaP-NPC10 + 10 % glucose	289.9 ± 18.9	303.6 ± 6.3

confirming the %EE data and the microscope observation. Similar release profiles were observed with C12DOXO as reported in a previous work (Chirio et al. 2022).

3.3. Human OSA cells in vitro studies

3.3.1. Cytotoxicity assay

To choose the concentrations of C12DOXO and CURC to be co-incubated when loaded into CaP-NPs, the concentration of each drug able to inhibit the cell proliferation by 50 % (IC50) was calculated after incubation of U-2OS and U-2OS/DX cell lines with drug solutions at concentration ranging from 0.01 to 100 μM.

The inhibition of cell proliferation induced by C12DOXO in OSA cells (Fig. 3) was different according to the cell line: in U-2OS IC50 of C12DOXO is relatively low (1.89 ± 0.17 μM) (Fig. 3A), while in DOXO resistant U-2OS/DX cells IC50 is higher than 100 μM (Fig. 3B). This difference is likely due to the overexpression of P-gp in U-2OS/DX cells that increases the efflux of DOXO from the cells.

On the contrary, the IC50 of CURC alone was 22.95 ± 1.36 μM and 23.64 ± 1.37 μM for U-2OS and U-2OS/DX, respectively (Fig. 4A and 4B). This result suggests that the cytotoxic effect of CURC, although less potent than that of DOXO, is independent of the presence of P-gp.

Consequently, 2.5 μM C12DOXO and 22 μM CURC were used in the following co-administration studies.

In Fig. 5, cell viability after 72-hour incubation with different samples (C12DOXO and CURC free or NP-loaded, alone or in combination) is reported.

Blank NPs (CaP-NP0), incubated at the same concentration of CaP-NPD6 2.5 μM + CaP-NPC10 22 μM, did not reduce cell viability, excluding that they can reduce cell viability. Cell viability was influenced both by drug loading and co-administration. Indeed, a significant

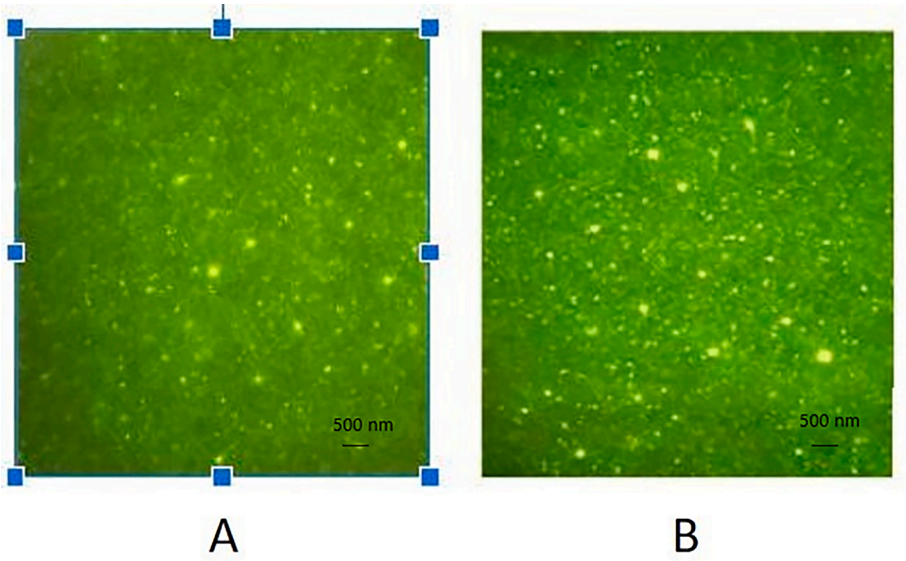

Fig. 1. Micrography of NPC10 (A) and CaP-NPC10 (B) at 1000 × magnification.

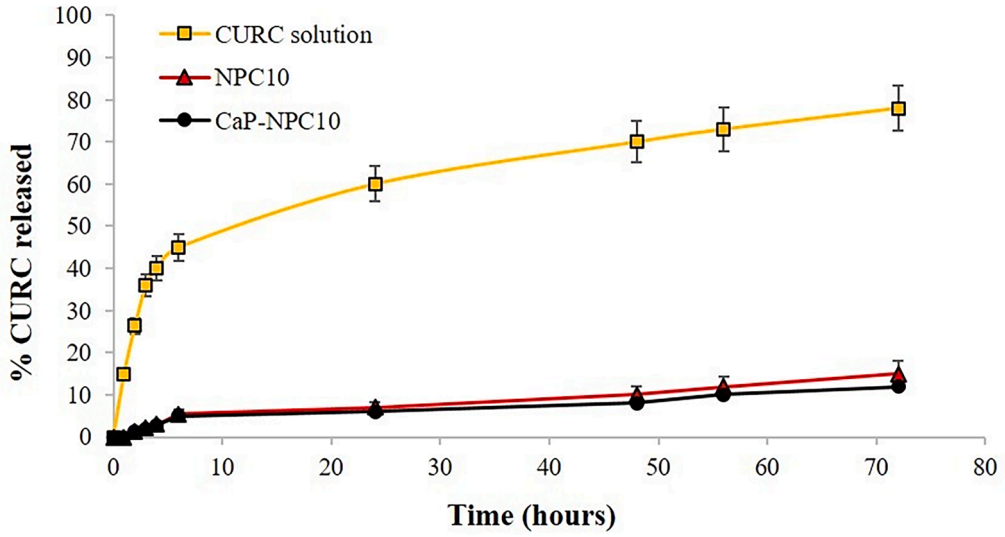

Fig. 2. CURC release profiles from: 10% w/w PEG 300 aqueous solution, NPC10, and CaP-NPC10.

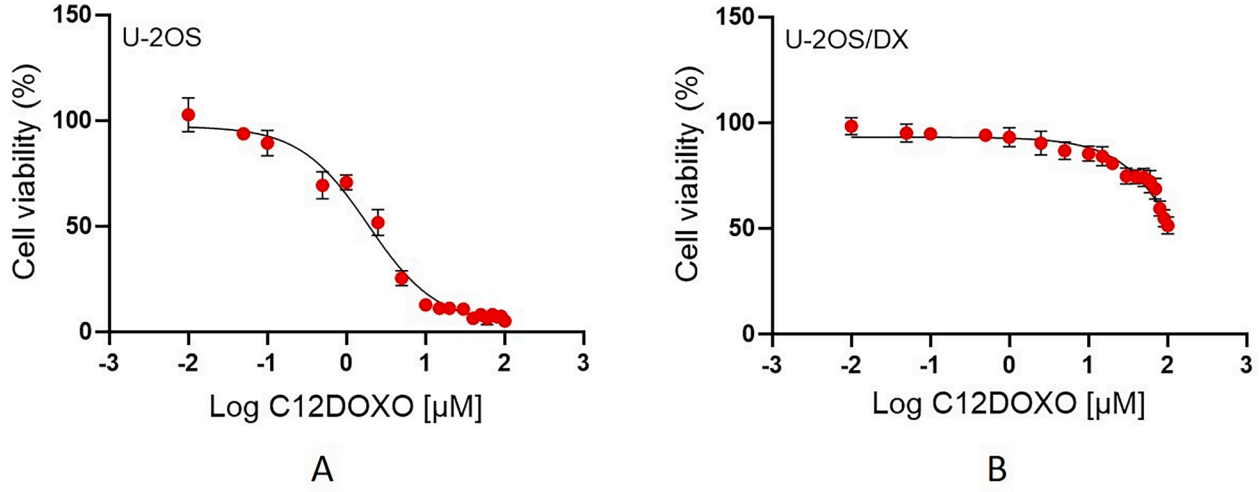

Fig. 3. The graphs represent the inhibition of cell proliferation induced by the administration of scalar concentrations (expressed as Log) of C12DOXO in OSA sensitive U-2OS (A) and OSA resistant cells U-2OS/DX (B). IC50 values were 1.89 ± 0.17 and > 100 μM for U-2OS and U-2OS/DX, respectively.

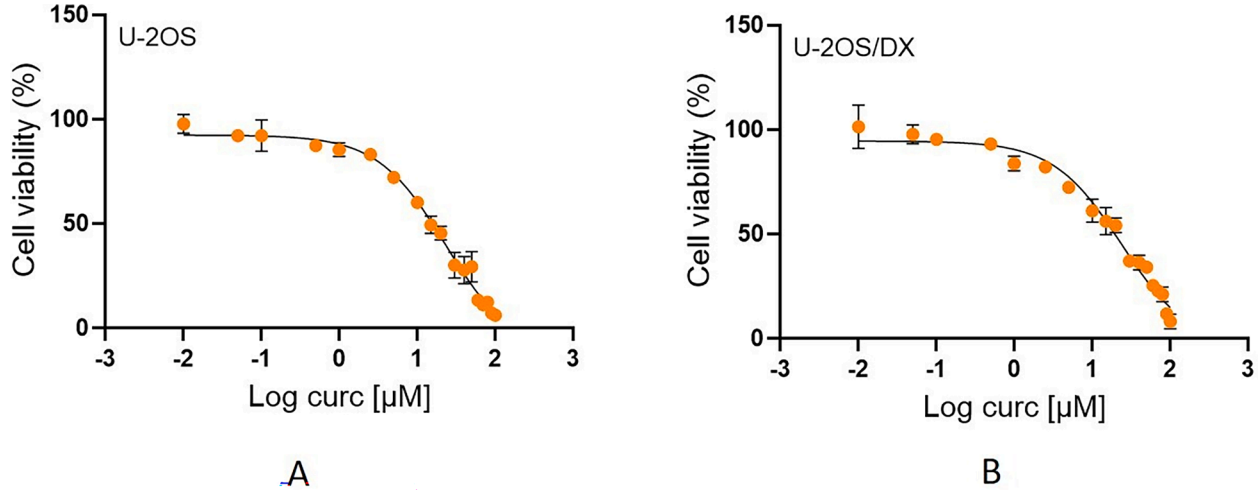

Fig. 4. The graphs represent the inhibition of cell proliferation induced by the administration of scalar concentrations (expressed as Log) of curcumin in OSA sensitive U-2OS (A) and OSA resistant cells U-2OS/DX (B). IC50 values were 22.95 ± 1,36 μM and 23.64 ± 1.37 μM for U-2OS and U-2OS/DX, respectively.

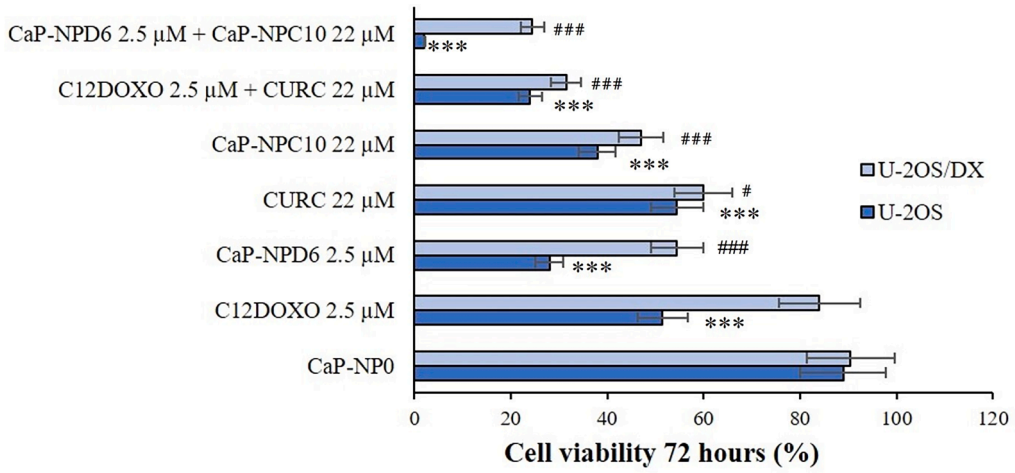

Fig. 5. Cell viability of U-2OS and U-2OS/DX cells incubated with different samples or with combination of samples for 72 h measured by MTT assay. Results are means ± SD (n = 4). For U-2OS cells: ***p < 0.001 (for all conditions except CaP-NP0) versus untreated cells, whose viability was considered 100 %. For U-2OS/DX cells: # p < 0.05: CURC 22 μM; ### p < 0.001 for CaP-NPD6 2.5 μM; CaP-NPC10 22 μM; C12DOXO 2.5 μM + CURC 22 μM; CaP-NPD6 2.5 μM + CaP-NPC10 22 μM versus untreated cells, whose viability was considered 100 %.

decrease of viability was observed when both CURC and C12DOXO were entrapped into NPs compared to free drugs but also when the two drugs were co-administered. As expected, in the U-2OS cell line the cell viability decreased up to 2 % when 2.5 μM CaP-NPD6 and 22 μM CaP-NPC10 were co-administered. The same trend was detected in U-2OS/DX cells even if the cell mortality was lower; in this case the co-administration of the two drugs loaded into NPs decreases the cell viability up to about 25 %. These results indicate the efficacy of CaP-NPs and CURC against DOXO-resistant human OSA cells. Since DOXO is an excellent substrate of P-gp, we next investigated whether the cytotoxic potential of the combination of CaP-NPD6 and CaP-NPC10 was due to an increased intracellular retention of DOXO caused by the inhibition of P-gp. The intracellular content of ATP, considered an index of viable cells, was measured as second parameter of cell viability (see supplementary Figure S1): the results were in line with the MTT assays and confirmed that CaP-NPD6 + CaP-NPC10 combination was the most effective in reducing cell viability in both DOXO-sensitive and DOXO-resistant cell lines.

Beside verifying that CaP formulations offer a significant advantage in terms of drug efficacy against drug resistant cells, an important issue when a new nanoformulation is used is to investigate the lack of adverse reactions on non-transformed cells. Hence, we tested the viability of human osteoblasts cells of free drugs and their formulations. As shown in Fig. 6 (MTT assay) and in supplementary Figure S2 (ATPLIte assay), neither free drugs (C12DOXO, CURC), nor their formulations, alone or combined, reduced cell viability to more than 30 %, demonstrating a lower effect on non-transformed cells. No significant differences were detected among the formulations, indicating that the presence of CaP does not significantly change the viability of non-transformed cells. The different behavior with tumor cells can be explained by a different pattern of endocytosis, release of the drug between cancer cells and non-transformed cells. To investigate this point, we thus measure the intracellular accumulation of DOX achieved in osteosarcoma and non-transformed osteoblasts.

3.3.2. *C12DOXO cellular uptake*

C12DOXO uptake data were consistent with cell viability results. Indeed, the amount of drug found in the cells increased when C12DOXO was loaded into CaP-NPs and when C12DOXO and CURC were co-administered. In detail, C12DOXO uptake in U2OS cells increased from 7 nmol/mg protein (C12DOXO solution) up to 23 nmol/mg protein (C12DOXO loaded in CaP-NPs and co-administered with CaP-NPC10).

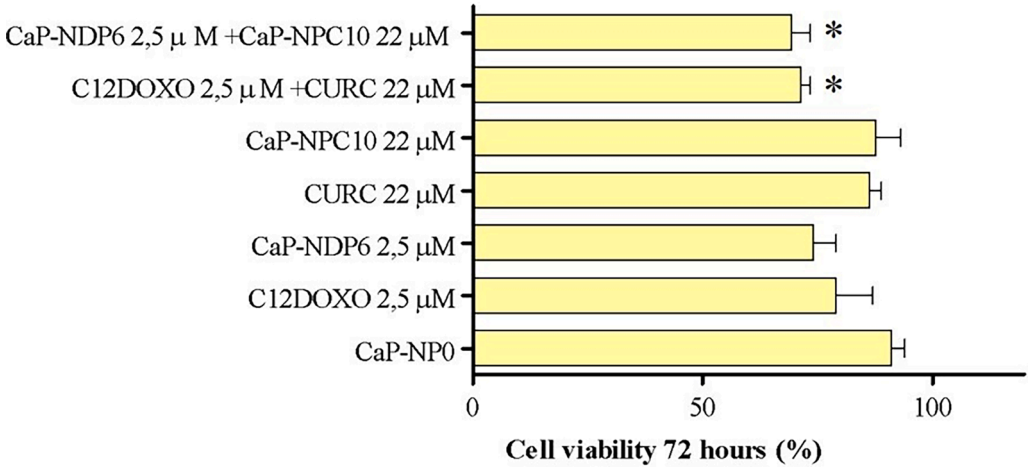

Fig. 6. Cell viability of human osteoblast cells incubated with different samples or with combination of samples for 72 h measured by MTT assay. Results are means ± SD. Significance: * p < 0.05 for C12DOXO 2.5 μM + CURC 22 μM; CaP-NPD6 2.5 μM + CaP-NPC10 22 μM versus untreated cells, whose viability was considered 100 %.

The same trend was noted in U-2OS/DX cell lines, where even a tenfold increase in drug uptake occurred comparing C12DOXO solution with C12DOXO loaded in CaP-NPs and co-administered with CaP-NPC10. However, in line with the higher levels of P-gp in the resistant cells, drug uptakes were lower (from 0.73 up to 7.5 nmol/mg protein) (Fig. 7A). Notably the uptake of C12DOXO and CaP-NPD6, alone or associated respectively with CURC or CaP-NPC10, was significantly lower in non-transformed osteoblasts (Fig. 7B), explaining the lower cytotoxicity observed. The same trend in terms of drug retention in U-2OS, U-2OS/DX and osteoblasts was confirmed by flow cytometry accumulation of the C12DOXO (Supplementary Figure S3). The differential profile of cytotoxicity and uptake of DOXO between osteosarcoma and non-transformed cells may set the basis for a potential therapeutic window in light of future applications in preclinical models *in vivo*.

To prove that the increased retention of DOXO was due to the P-gp inhibition, we co-incubated verapamil, an inhibitor of P-gp, with free C12DOXO, CaP-NPD6 and CaP-NPD6 + CaP-NPC10. Verapamil increased the retention of C12DOXO in a time dependent manner. The effects were greater in U-2OS/DX, which express higher amounts of P-gp than in U2-2OS (Buondonno et al., 2019). In DOXO-resistant cells, the benefit of verapamil followed this rank order: CaP-NPD6 + CaP-NPC10 > CaP-NPD6 > free C12DOXO. This trend suggests that C12DOXO might be a substrate of P-gp in OSA cells, but its entrapment in CaP-NPs likely makes the drug less subject to the efflux of P-gp. The presence of CaP-NPC10 offers a further advantage, because the entrapment of CUR in NPs, granting a higher bioavailability of the compound, enhances its effect as P-gp inhibitor, in line with previous results obtained in TNBC (Fathy Abd-Ellatef et al., 2020). The triple combination of verapamil plus CaP-NPD6 and CaP-NPC10 achieved the highest intracellular retention of drug, because of the double inhibition – exerted by CUR and verapamil, on P-gp (Fig. 8).

3.4. Canine OSA cells in vitro studies

3.4.1. Cytotoxicity assay

As previously exposed for the human counterpart, also for D17 cell line a range of concentrations from 0.01 to 100 μM of C12DOXO and CURC has been tested. After 72 h incubation, MTT assay was performed. Data have been analyzed in order to calculate IC50, which was subsequently used to proceed to further experimental steps. In Fig. 9, D17 cell viability after 72 h incubation with C12DOXO is reported, while in Fig. 10 the response to CURC incubation is reported. IC50 values were 58.92 ± 0.2191 μM and 16.43 ± 0.1855 μM, respectively.

According to the results obtained in the present experimental setting, the responses of the D17 cell line were completely different to the two compounds. The trend of C12DOXO showed an initial decrease in cell proliferation, reaching the lowest percentage of cell viability at the concentration of 2.5 μM. The concentrations of 5 and 10 μM demonstrated a slight increase in cell proliferation but a dramatic and significant increase was shown from the concentration of 15 μM to the

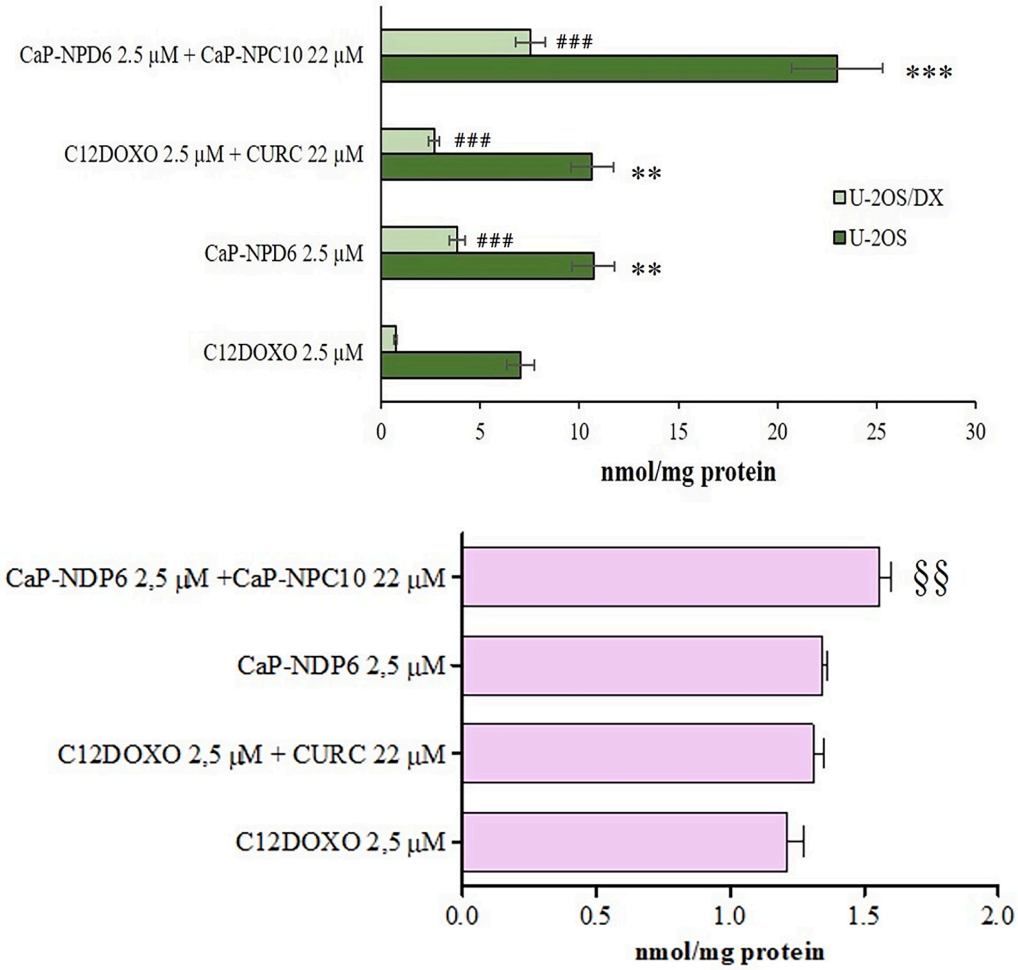

Fig. 7. Uptake of C12DOXO in U-2OS and in U-2OS/DX cells (Panel A) and in non-transformed osteoblasts (panel B) 24 h after sample incubation. Results are means ± SD (n = 4). For U-2OS cells: ** $p < 0.01$ for CaP-NPD6 2.5 μM/CaP-NPD6 2.5 μM + CURC 22 μM vs C12DOXO; *** $p < 0.001$ for CaP-NPD6 2.5 μM + CaP-NPC10 22 μM vs C12DOXO. For U-2OS/DX cells: ### $p < 0.001$ for all conditions vs C12DOXO. For non-transformed osteoblasts: §§ $p < 0.01$: CaP-NPD6 2.5 μM + CURC 22 μM vs C12DOXO.

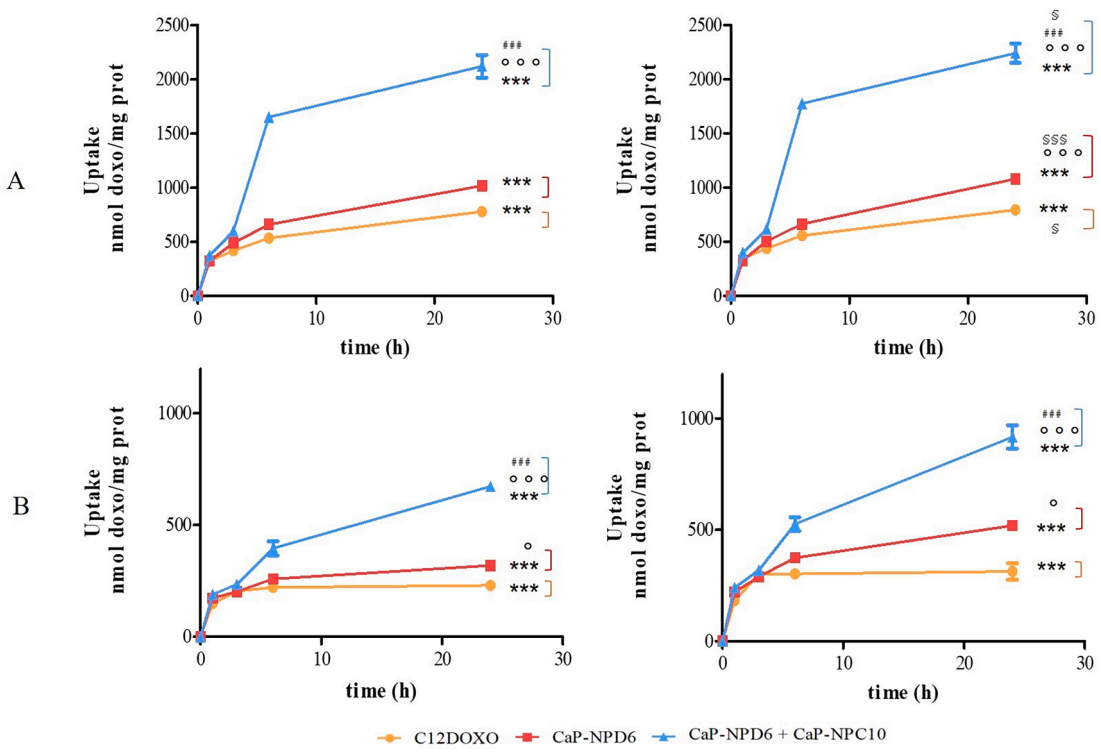

Fig. 8. Uptake of C12DOXO 24 h after sample incubation in the absence (left) and in the presence (right) of verapamil in U-2OS (A) and U-2OS/DX (B) cells. Results are means ± SD (n = 4). *p < 0.05, **p < 0.01, ***p < 0.001: 24 h vs 1 h; °p < 0.05, °°p < 0.01, °°°P < 0.001: vs C12DOXO; #p < 0.05, ##p < 0.01, ###P < 0.001: vs CAP-NPD6; §p < 0.05, §§p < 0.01, §§§P < 0.001: vs no verapamil.

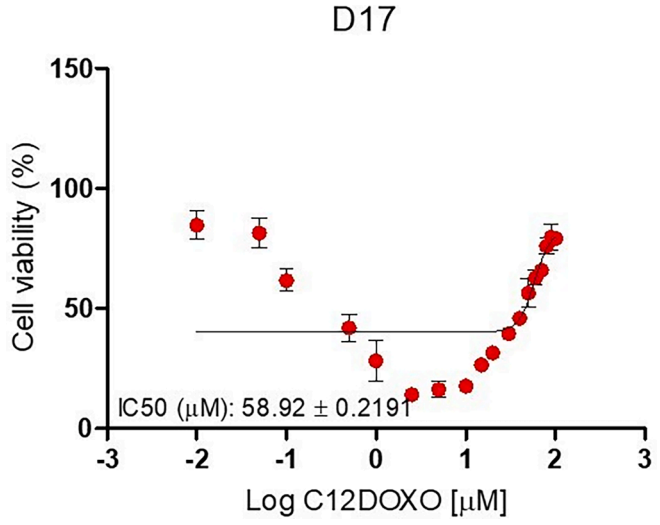

Fig. 9. The graph represents the inhibition of cell proliferation induced by the administration of scalar concentrations (expressed as Log) of C12DOXO in OSA canine cell line, D17. IC50 value was 58.92 ± 0.2191 µM.

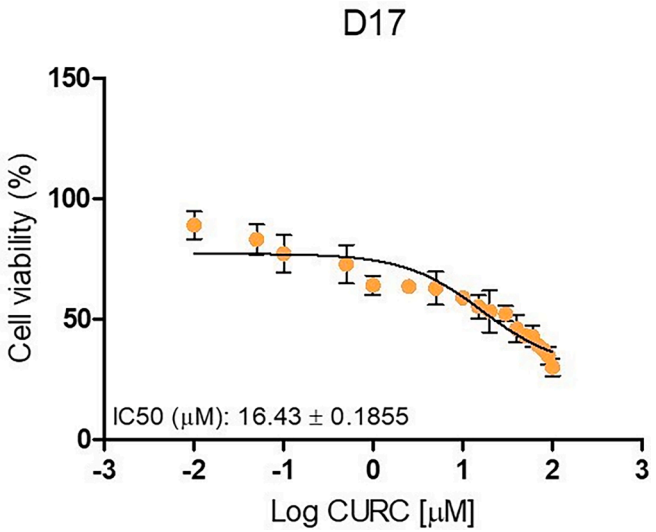

Fig. 10. The graph represents the inhibition of cell proliferation induced by the administration of scalar concentrations (expressed as Log) of CURC in OSA canine cell line, D17. IC50 value was 16.43 ± 0.1855 µM.

maximum concentration of 100 µM. This particular behavior could be motivated considering that the highest concentrations may induce an alteration of the transport systems due to a saturation after the long incubation period or an increased activity of the efflux pump may be induced. For the following experimental steps, the IC50 of 59 µM has been considered for the incubation of C12DOXO in D17 cell line.

On the contrary, the response of D17 cell line after 72 h incubation with CURC demonstrated a concentration-dependent behavior.

IC50 value was calculated as 16.43 ± 0.1855 µM, and the concentration equal to 16 µM has been chosen for further experimental steps.

In Fig. 11 and in supplementary Figure S4 cell viability after 72 h incubation with different samples (C12DOXO and CURC free or NP-loaded, alone or in combination), obtained by MTT test and ATPlite assay respectively, is reported.

The highest rate of cytotoxicity was demonstrated for the association of CaP-NPD6 59 µM + CaP and NPC10 16 µM. Nevertheless, no statically significant differences have been appreciated with the association of C12DOXO 59 µM and CURC 16 µM: this result suggests that the combination between DOXO and CURC must be pursuit because both compounds, administered together, can significantly improve the inhibition

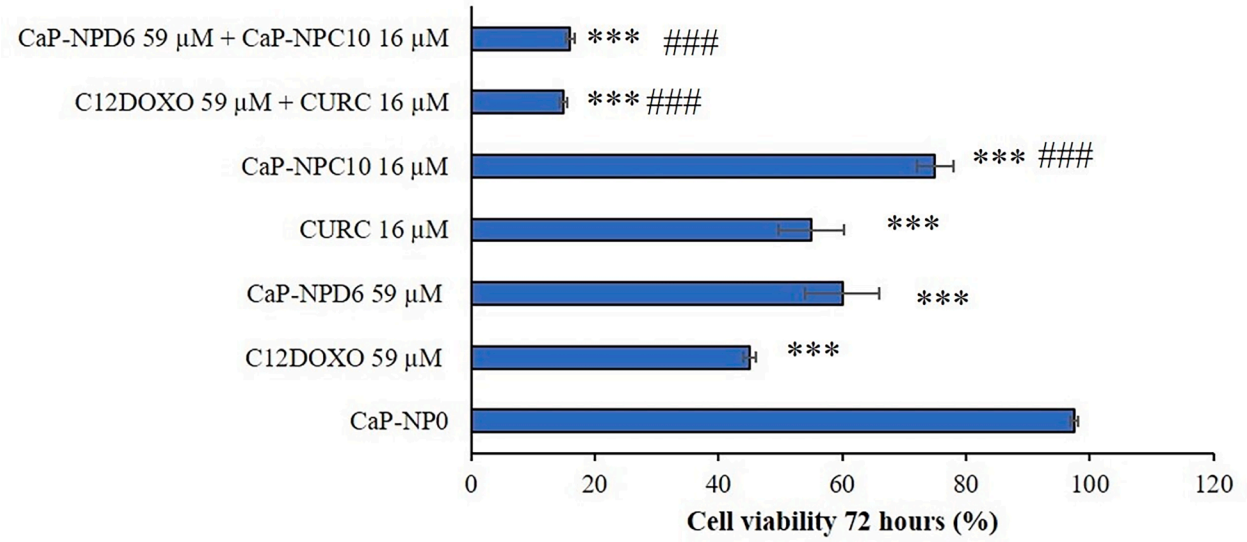

Fig. 11. Cell viability of D17 cells incubated with different samples or with combination of samples for 72 h measured by MTT assay. Results are means ± SD (n = 5). ***p < 0.001 for all conditions except CaP-NP0 and CaP-NPC10 16 µM versus untreated cells, whose viability was considered 100 %. ### p < 0.001 versus C12DOXO 59 µM.

of proliferation of OSA in a canine model. This hypothesis find confirmation considering the data obtained by the single compounds tested alone: CURC in both formulations is not able to induce any significant inhibition of cell proliferation, while DOXO at the concentration used in the present experimental setting was able to induce a more evident inhibition of cell growth but without reaching the values obtained by the association. Blank NPs (CaP-N0) did not induce any statistical significant alteration of cell proliferation.

3.4.2. C12DOXO cellular uptake

In Fig. 12 C12DOXO cellular uptake data are reported.

The results obtained in the cellular uptake assay showed that the highest rate of uptake was obtained with CaP-NPD6 59 µM. This value was significantly different compared to other samples or associations. Nevertheless, also the association of CaP-NPD6 and CaP-NPC10 showed a value of uptake, higher than that reported for the association C12DOXO 59 µM + CURC 16 µM. It is possible that the discrepancy between viability and uptake of CaP-NPD6 (Figs. 11 and 12, respectively) might be explained by the fact that NPs enter the cell as a whole and release the drug there slowly even after 72 h. A prolonged release within the cell could therefore be obtained, resulting in a reduction in the frequency of administration. Once again, the intracellular DOXO accumulation measured by flow cytometry confirmed the results obtained by fluorometric quantification (Supplementary Figure S5).

Considering that the association seems to decrease the uptake of C12DOXO-loaded NPs pushed to carefully evaluate possible specific cellular mechanisms. For this reason, also for D17 cells, an experimental setting using verapamil has been set (Fig. 13).

The co-incubations were made by adding verapamil to free C12DOXO, CaP-NPD6 and CaP-NPD6 + CaP-NPC10. Verapamil increased the uptake of all tested formulations, and it was possible to appreciate the following: CaP-NPD6 + CaP-NPC10 > CaP-NPD6 > free C12DOXO. Similar to what has been already written about the human OSA cell lines, this behavior is explainable considering that C12DOXO might be is a substrate of P-gp and that its entrapment in CaP-NPs might

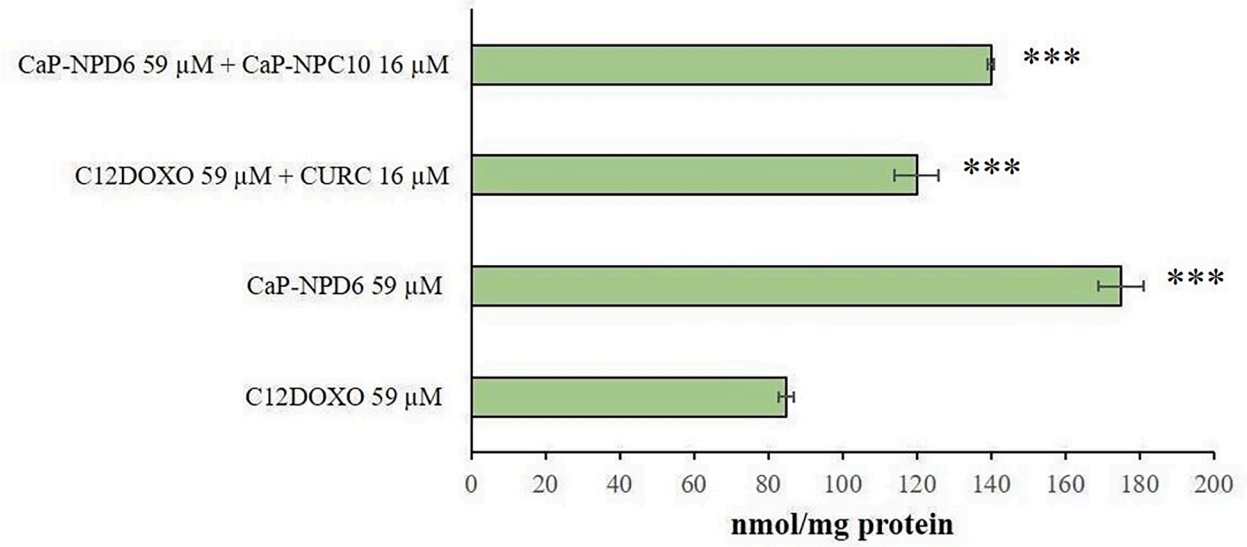

Fig. 12. Uptake of C12DOXO in D17 24 h after sample incubation. Results are means ± SD (n = 5). *** p < 0.001 for all comparisons vs C12DOXO 59 µM.

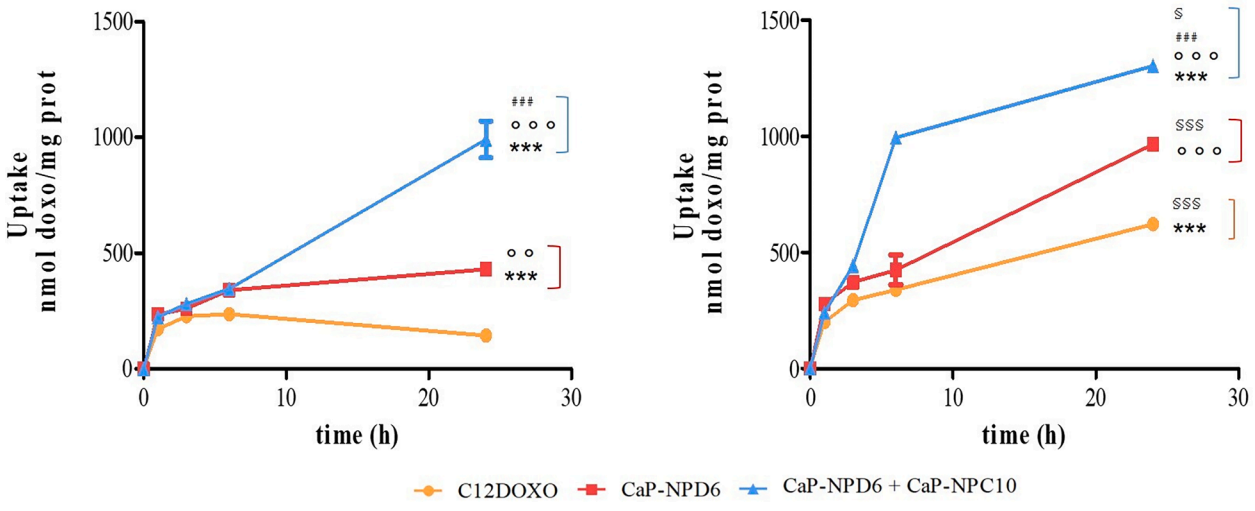

Fig. 13. Uptake of C12DOXO in D17 cells, 24 h after sample incubation, in the absence (left) and in the presence (right) of verapamil. Results are means ± SD (n = 4). $p < 0.05$, $^{**}p < 0.01$, $^{***}p < 0.001$: 24 h vs 1 h; $^{\circ}p < 0.05$, $^{\circ\circ}p < 0.01$, $^{\circ\circ\circ}P < 0.001$: vs C12DOXO; $\#p < 0.05$, $\#\#p < 0.01$, $\#\#\#P < 0.001$: vs CAP-NPD6; $\S p < 0.05$, $\S\S p < 0.01$, $\S\S\S P < 0.001$: vs no verapamil.

made the drug less subject to the efflux of P-gp. The data about the increased uptake of the formulation containing CURC are encouraging and seem to suggest that the uptake is significantly improved when P-gp efflux is inhibited. These results and observations are in accordance with a previous description of the presence of efflux pump in D17 cells: another investigation already demonstrated that verapamil is able to increase intracellular accumulation of DOXO by inhibiting P-gp transporter mechanism (Małek et al. 2021).

The effectiveness of cancer treatments has significantly improved in the last decades due to the advancement in early diagnosis and treatments. Nevertheless, the chemotherapy still relies on cytotoxic chemotherapy. The natural evolution of the investigation to find new successful treatments rely on the possibility to improve the actual formulation or to renew the interest in natural compounds (Wagle, et al., 2024).

The importance of using canine tumors as models for human species is an interesting topic that can provide more useful information compared to those obtainable from murine tumor models. Canine OSA share many biological, genetic, and histologic features with their human tumor counterparts, and retain the complexities of naturally occurring drug resistance, metastasis, and tumor-host immune interactions (Klosowsk et al., 2023). Genomic descriptions of OSA are increasingly frequent, supporting the shared chromosomal, genetic, and epigenetic abnormalities between dog and human. Carefull analysis such as whole genome, transcriptome, and methylome sequencing were used to identify similar alteration between human and canine OSA such as chromosomal rearrangements, gene mutations, alterations in gene expression, alterations in microRNA expression, and DNA methylation (Bryan, 2024). In a hypothetical scenario, the canine OSA model might facilitate treatment advances benefitting both species. Nevertheless, some limitations exist in real clinical practice and also some inherent differences must be considered (Klosowski et al., 2023). In fact, considering the results obtained in the present study, it appears that the results of the *in vitro* evaluations of human and canine cell lines are not completely comparable. The MTT assay in the presence of C12DOXO showed that D17 cell line demonstrated an initial decrease of cell proliferation, followed by a subsequent increase at higher concentrations (Fig. 11). This different biological behavior is not surprising, since it was already reported in literature that human and canine cell lines can exhibit different responses to pharmacological treatments (Vercelli et al. 2015). This should always be taken into consideration when studies about comparative oncology are planned. Even if the macroscopic presentation and the histologic examination seem to suggest that the human and canine neoplasms are very similar (or almost identical) the underlying molecular mechanisms may be completely different. In Author's opinion, the data reported in the present manuscript seem to suggest that human and canine OSA cell lines can react differently to the incubation of C12DOXO and CURC NPs. Indeed, a recent paper dealing with human and canine OSA reported that the viability of D17 cell line was less affected by the incubation of DOXO, cisplatin and etoposide alone if compared to human cell cultures, while their combinations appeared to induce a strongest effect (Poradowski et al. 2022).

4. Conclusions

Our previous works showed that the use of CaP-coated NPs can play a key role in enhancing the retention of C12DOXO in human and canine OSA cells. Building on these findings, the primary objective of the present study was to investigate whether co-incubation of C12DOXO-loaded CaP-NPs with CURC-loaded CaP-NPs could serve as an effective strategy to further increase drug uptake and, consequently, enhance the cytotoxicity of DOXO in OSA cell lines from both species.

In vitro cell studies on C12DOXO-loaded NPs and CURC-loaded NPs, tested alone and in combination, evidenced different biological behaviors into human and canine cells. In human U-2OS cells, as well as in DOXO resistance U-2OS cells, both CURC and C12DOXO induced a higher decrease of cell viability when entrapped into CaP-NPs compared to the corresponding free drugs. Also in canine D17 cells the positive effect of co-incubation was observed, and differences in biological response have been highlighted in comparison with the human OSA cell lines.

Moreover, a greater cytotoxicity was observed when the drugs were co-incubated both in the free form and loaded in NPs. The efficacy of C12DOXO-loaded NPs against P-gp expressing human osteosarcoma is of particular importance in a translational perspective, because the level of P-gp is a biomarker predictive of a faster progression and poor response to chemotherapy (Pakos and Ioannidis, 2003). Rescuing the efficacy of DOXO, the first-line drug in this tumor, also in OSA expressing P-gp, for instance using NP formulations and combination treatments, represents an advance in the treatment strategies of OSA patients. In conclusion, the here proposed approach holds significant potential for both human and veterinary medicine, warranting further investigation.

CRediT authorship contribution statement

Simona Sapino: Writing – review & editing, Writing – original draft, Conceptualization. **Elena Peira:** Methodology, Investigation. **Daniela Chirio:** Validation, Data curation, Conceptualization. **Giulia Chindamo:** Software, Formal analysis. **Giulia Accomasso:** Software, Formal analysis. **Cristina Vercelli:** Writing – review & editing, Validation, Methodology. **Chiara Riganti:** Validation, Supervision, Data curation. **Iris Chiara Salaroglio:** Methodology, Formal analysis. **Graziana Gambino:** Writing – original draft, Software. **Giovanni Re:** Supervision, Data curation. **Michela Amadori:** Software, Formal analysis. **Marina Gallarate:** Writing – review & editing, Supervision.

Funding

"This research received no external funding".
Institutional Review Board Statement: "Not applicable".
Informed Consent Statement: "Not applicable.".

Declaration of competing interest

The authors declare that they have no known competing financial interests or personal relationships that could have appeared to influence the work reported in this paper.

Appendix A. Supplementary data

Supplementary data to this article can be found online at https://doi.org/10.1016/j.ijpharm.2024.124970.

Data availability

Data will be made available on request.

References

Anuchapreeda, S., Leechanachai, P., Smith, M.M., Ambudkar, S.V., Limtrakul, P., 2002. Modulation of P-glycoprotein expression and function by curcumin in multidrug-resistant human KB cells. Biochem. Pharmacol. 64, 573–582. https://doi.org/10.1016/s0006-2952(02)01224-8.

Barraud, L., Merle, P., Soma, E., Lefrançois, L., Guerret, S., Chevallier, M., Vitvitski, L., 2005. Increase of doxorubicin sensitivity by doxorubicin-loading into nanoparticles for hepatocellular carcinoma cells in vitro and in vivo. J. Hepatol. 42, 736–743. https://doi.org/10.1016/j.jhep.2004.12.035.

Bryan, J.N., 2024. Updates in Osteosarcoma. *The Veterinary Clinics of North America.* Small Animal Practice 54 (3), 523–539. https://doi.org/10.1016/j.cvsm.2023.12.007.

Buondonno, I., Gazzano, E., Jean, S.R., Audrito, V., Kopecka, J., Fanelli, M., Salaroglio, I. C., Costamagna, C., Roato, I., Mungo, E., Hattinger, C.M., Deaglio, S., Kelley, S.O., Serra, M., Riganti, C., 2016. Mitochondria-targeted doxorubicin: a new therapeutic strategy against doxorubicin-resistant osteosarcoma. Mol. Cancer Ther. 15, 2640–2652. https://doi.org/10.1158/1535-7163.MCT-16-0048.

Buondonno, I., Gazzano, E., Tavanti, E., Chegaev, K., Kopecka, J., Fanelli, M., Rolando, B., Fruttero, R., Gasco, A., Hattinger, C., Serra, M., Riganti, C., 2019. Endoplasmic reticulum-targeting doxorubicin: a new tool effective against doxorubicin-resistant osteosarcoma. Cell Mol Life Sci. 76, 609–625. https://doi.org/10.1007/s00018-018-2967-9.

Chirio, D., Peira, E., Dianzani, C., Muntoni, E., Gigliotti, C.L., Ferrara, B., Sapino, S., Chindamo, G., Gallarate, M., 2019. Development of solid lipid nanoparticles by cold dilution of microemulsions: curcumin loading, preliminary in vitro studies, and biodistribution. Nanomaterials 9, 230, 10.3390%2Fnano9020230.

Chirio, D., Sapino, S., Chindamo, G., Peira, E., Vercelli, C., Riganti, C., Manzoli, M., Gambino, G., Re, G., Gallarate, M., 2022. Doxorubicin-loaded lipid nanoparticles coated with calcium phosphate as a potential tool in human and canine osteosarcoma therapy. Pharmaceutics 14, 1362. https://doi.org/10.3390/pharmaceutics14071362.

Duggan, S.T., Keating, G.M., 2011. Pegylated liposomal doxorubicin. Drugs 71, 2531–2558. https://doi.org/10.2165/11207510-000000000-00000.

Fathy Abd-Ellatef, G.E., Gazzano, E., Chirio, D., Hamed, A.R., Belisario, D.C., Zuddas, C., Peira, E., Rolando, B., Kopecka, J., Marie, A.S.M., Sapino, S., Ramadan Fahmy, S., Gallarate, M., Abdel-Hamid, A.Z., Riganti, C., 2020. Curcumin-loaded solid lipid nanoparticles bypass p-glycoprotein mediated doxorubicin resistance in triple negative breast cancer cells. Pharmaceutics 12, 96. https://doi.org/10.3390/pharmaceutics12020096.

Garcia-Ortega, D.Y., Cabrera-Nieto, S.A., Caro-Sánchez, H.S., Cruz-Ramos, M., 2022. An overview of resistance to chemotherapy in osteosarcoma and future perspectives. Cancer Drug Resist. 5, 762–793. https://doi.org/10.20517/cdr.2022.18.

Gazzano, E., Buondonno, I., Marengo, A., Rolando, B., Chegaev, K., Kopecka, J., Saponara, S., Sorge, M., Hattinger, C.M., Gasco, A., Fruttero, R., Brancaccio, M., Serra, M., Stella, B., Fattal, E., Arpicco, S., Riganti, C., 2019. Hyaluronated liposomes containing H2S-releasing doxorubicin are effective against P-glycoprotein-positive/doxorubicin-resistant osteosarcoma cells and xenografts. Cancer Letters 456, 29–39. https://doi.org/10.1016/j.canlet.2019.04.029.

Gronthos, S., Zannettino, A.C., Hay, S.J., Shi, S., Graves, S.E., Kortesidis, A., Simmons, P. J., 2003. Molecular and cellular characterisation of highly purified stromal stem cells derived from human bone marrow. Journal of Cell Science 116 (Pt 9), 1827–1835. https://doi.org/10.1242/jcs.00369.

Kciuk, M., Gielecińska, A., Mujwar, S., Kołat, D., Kałuzińska-Kołat, Ż., Celik, I., Kontek, R., 2023. Doxorubicin An agent with multiple mechanisms of anticancer activity. Cells. 12, 659. https://doi.org/10.3390/cells12040659.

Klosowski, M., Haines, L., Alfino, L., McMellen, A., Leibowitz, M., Regan, D., 2023. Naturally occurring canine sarcomas: Bridging the gap from mouse models to human patients through cross-disciplinary research partnerships. Frontiers in Oncology 13, 1130215. https://doi.org/10.3389/fonc.2023.1130215.

Lee, D.S., Lee, M.K., Kim, J.H., 2009. Curcumin Induces Cell Cycle Arrest and Apoptosis in Human Osteosarcoma (HOS) Cells. Anticancer Res 29, 5039–5044. https://ar.iiarjournals.org/content/anticanres/29/12/5039.full.pdf.

Li, S., Sun, W., Wang, H., Zuo, D., Hua, Y., Cai, Z., 2015. Research progress on the multidrug resistance mechanisms of osteosarcoma chemotherapy and reversal. Tumour Biol. 36, 1329–1338. https://doi.org/10.1007/s13277-015-3181-0.

Makielski, K.M., Mills, L.J., Sarver, A.L., Henson, M.S., Spector, L.G., Naik, S., Modiano, J.F., 2019. Risk factors for development of canine and human osteosarcoma: a comparative review. Vet. Sci. 6, 48. https://doi.org/10.3390/vetsci6020048.

Małek, A., Taciak, B., Sobczak, K., Grzelak, A., Wójcik, M., Mieczkowski, J., Lechowski, R., Zabielska-Koczywąs, K.A., 2021. Enhanced cytotoxic effect of doxorubicin conjugated to glutathione-stabilized gold nanoparticles in canine osteosarcoma—in vitro studies. Molecules 26, 3487. https://doi.org/10.3390/molecules26123487.

Pakos, E.E., Ioannidis, J.P., 2003 Aug 1. The association of P-glycoprotein with response to chemotherapy and clinical outcome in patients with osteosarcoma. A Meta-Analysis. Cancer. 98 (3), 581–589. https://doi.org/10.1002/cncr.11546. PMID: 12879476.

Peira, E., Chirio, D., Battaglia, L., Barge, A., Chegaev, K., Gigliotti, C.L., Ferrara, B., Dianzani, C., Gallarate, M., 2016. Solid lipid nanoparticles carrying lipophilic derivatives of doxorubicin: Preparation, characterization, and in vitro cytotoxicity studies. J Microencapsul 33, 381–390. https://doi.org/10.1080/02652048.2016.1202342.

Petschauer, J.S., Madden, A.J., Kirschbrown, W.P., Song, G., Zamboni, W.C., 2015. The effects of nanoparticle drug loading on the pharmacokinetics of anticancer agents. Nanomedicine 10, 447–463. https://doi.org/10.2217/nnm.14.179.

Poradowski, D., Chrószcz, A., Obmińska-Mrukowicz, B., 2022. Synergistic antitumor interaction of risedronate sodium and standard anticancer agents in canine (D-17) and human osteosarcoma (U-2 OS) Cell Lines. Animals 12, 866. https://doi.org/10.3390/ani12070866.

Rana, A., Adhikary, M., Singh, P.K., Das, B.C., Bhatnagar, S., 2023. "Smart" drug delivery: A window to future of translational medicine. Front. Chem. 10, 1095598. https://doi.org/10.3389/fchem.2022.1095598.

Sapino, S., Chindamo, G., Chirio, D., Manzoli, M., Peira, E., Riganti, C., Gallarate, M., 2021. Calcium phosphate-coated lipid nanoparticles as a potential tool in bone diseases therapy. Nanomaterials 11, 2983. https://doi.org/10.3390/nano11112983.

Serra, M., Scotlandi, K., Manara, M.C., Maurici, D., Lollini, P.L., De Giovanni, C., Toffoli, G., Baldini, N., 1993. Establishment and characterization of multidrug-resistant human osteosarcoma cell lines. Anticancer Res. 13, 323–329. https://pubmed.ncbi.nlm.nih.gov/8100126/.

Sheibani, M., Azizi, Y., Shayan, M., Nezamoleslami, S., Eslami, F., Farjoo, M.H., Dehpour, A.R., 2022. Doxorubicin-induced cardiotoxicity: an overview on pre-clinical therapeutic approaches. Cardiovasc Toxicol. 22, 292–310. https://doi.org/10.1007/s12012-022-09721-1.

Sun, K., Yuan, L., Chen, S., Sun, Y., Wei, D. 2024 Alendronate PtIV prodrug amphiphile for enhanced chemotherapy targeting and bone destruction inhibition in osteosarcoma. Adv Healthc Mater. Mar 13, e2302746. doi: 10.1002/adhm.202302746.

Sun, Y., Liu, L., Wang, Y., He, A., Hu, H., Zhang, J., et al., 2019. Curcumin inhibits the proliferation and invasion of MG-63 cells through inactivation of the p-JAK2/p-STAT3 pathway. Onco. Targets Ther. 12, 2011–2021. https://doi.org/10.2147/OTT.S172909.

Susa, M., Iyer, A.K., Ryu, K., Choy, E., Hornicek, F.J., Mankin, H., et al., 2010. Inhibition of ABCB1 (MDR1) expression by an siRNA nanoparticulate delivery system to overcome drug resistance in osteosarcoma. PLoS ONE 5, e10764. Doi: 10.1371/journal.pone.0010764.

Susa, M., Iyer, A.K., Ryu, K., Hornicek, F.J., Mankin, H., Amiji, M.M., Duan, Z., 2009. Doxorubicin loaded polymeric nanoparticulate delivery system to overcome drug resistance in osteosarcoma. BMC Cancer 9, 1–12. https://doi.org/10.1186/1471-2407-9-399.

Swain, S.M., Whaley, F.S., Ewer, M.S., 2003. Congestive heart failure in patients treated with doxorubicin: A retrospective analysis of three trials. Cancer 97, 2869–2879. https://doi.org/10.1002/cncr.11407.

Ta, H.T., Dass, C.R., Choong, P.F.M., Dunstan, D.E., 2009. Osteosarcoma treatment: state of the art. Cancer Metastasis Rev. 28, 247–263. https://doi.org/10.1007/s10555-009-9186-7.

Tang, X.q., Bi, H., Feng, J.q., et al., 2005. Effect of curcumin on multidrug resistance in resistant human gastric carcinoma cell line SGC7901/VCR. Acta Pharmacol. Sin. 26, 1009–1016. https://doi.org/10.1111/j.1745-7254.2005.00149.x.

Trotta, M., Peira, E., Carlotti, M.E., Gallarate, M., 2004. Deformable liposomes for dermal administration of methotrexate. Int. J. Pharm. 270, 119–125. https://doi.org/10.1016/j.ijpharm.2003.10.006.

Vercelli, C., Barbero, R., Cuniberti, B., Racca, S., Abbadessa, G., Piccione, F., Re, G., 2014. Transient receptor potential vanilloid 1 expression and functionality in MCF-7 cells: A preliminary investigation. J. Breast Cancer 17, 332–338. https://doi.org/10.4048/jbc.2014.17.4.332.

Vercelli, C., Barbero, R., Cuniberti, B., Odore, R., Re, G., 2015. Expression and functionality of TRPV1 receptor in human MCF-7 and canine CF.41 cells. Vet. Comp. Oncol. 13, 133–142. https://doi.org/10.1111/vco.12028.

Wagle, S., Lee, J.A., Rupasinghe, H.P.V., 2024. Synergistic cytotoxicity of extracts of Chaga mushroom and microalgae against mammalian cancer cells in vitro. *Oxidative Medicine and Cellular Longevity* 2024, 7944378. https://doi.org/10.1155/2024/7944378.

Walters, D.K., Muff, R., Langsam, B., et al., 2008. Cytotoxic Effects of Curcumin on Osteosarcoma Cell Lines. Invest. New Drugs 26, 289–297. https://doi.org/10.1007/s10637-007-9099-7.

Wang, L., Wang, W.G., Rui, Z., Zhou, D.S., 2016. The effective combination therapy against human osteosarcoma: doxorubicin plus curcumin co-encapsulated lipid-coated polymeric nanoparticulate drug delivery system. Drug Deliv. 23, 3200–3208. https://doi.org/10.3109/10717544.2016.1162875.

Withers, S.S., York, D., Johnson, E., Al-Nadaf, S., Skorupski, K.A., Rodriguez, C.O., et al., 2018. In vitro and in vivo activity of liposome-encapsulated curcumin for naturally occurring canine cancers. Vet. Comp. Oncol. 16, 571–579. https://doi.org/10.1111/vco.12424.

Xue, X., Yu, J., Sun, D., Zou, W., Kong, F., Wu, J., Liu, H., Qu, X., Wang, R., 2013. Curcumin as a multidrug resistance modulator — A quick review. Biomedicine & Preventive Nutrition 3, 173–176. https://doi.org/10.1016/j.bionut.2012.12.001.

Zhang, Y., Chen, P., Hong, H., Wang, L., Zhou, Y., Lang, Y., 2017. JNK pathway mediates curcumin-induced apoptosis and autophagy in osteosarcoma MG63 cells. Exp. Ther. Med. 14, 593–599. https://doi.org/10.3892/etm.2017.4529.